ATS/Note/2011/068 TECH

August 31, 2011

ketil.roeed@cern.ch

Application benchmark and comparison of the LHC Radiation Monitor and FLUKA Monte Carlo simulations in IR7

Ketil Røed / EN-STI, Vittorio Boccone / EN-STI, Markus Brugger / EN-STI, Marco Calviani / EN-STI, Francesco Cerutti / EN-STI, Alfredo Ferrari / EN-STI, Daniel Kramer / EN-STI, Elias Lebbos / EN-STI, Anton Lechner / EN-STI, Roberto Losito / EN-STI, Alessio Mereghetti / EN-STI, David Sinuela Pastor / EN-STI, Giovanni Spiezia / EN-STI, Adam Thornton / EN-STI, Roberto Versaci / EN-STI, Vasilios Vlachoudis / EN-STI,

Keywords: LHC, R2E, RadMon, FLUKA, SEU

Summary

At the LHC various underground areas are partly equipped with commercial electronic devices not specifically designed to be radiation tolerant. A major concern is therefore radiation induced failures in particular due to Single Event Upsets (SEU). To ensure safe and acceptable operation of the LHC electronics a combination of both FLUKA Monte Carlo simulations and dedicated online monitoring is applied to determine the expected radiation levels in critical areas. The LHC Radiation Monitor (RadMon) which is used for this purpose has already been extensively calibrated for its radiation response in various irradiation facilities. It is nevertheless of high importance to also provide a real LHC application benchmark to validate the approach of combined simulations and monitoring to correctly measure and predict radiation levels. This report therefore presents a comparison between FLUKA [1, 2] Monte Carlo simulations and measurements results using the RadMon in the LHC collimation region IR7. The work is carried out within the frame work of the R2E project.

1 Introduction

At the LHC various areas are partly equipped with commercial electronic devices not specifically designed to be radiation tolerant. The main sources of radiation relevant for radiation effects in electronics at the LHC are direct losses in collimators and collimator like objects, particle debris from proton-proton or lead-lead collisions in the four main experiments, and interaction of the beam with the residual gas inside the beam pipe. The result is a complex radiation field of mixed particle types and energies. One of the major concerns is operational failures induced by Single Event Upsets (SEUs). An SEU is a bit flip in a memory cell induced by the deposited charge from one ionizing particle transversing the memory cell. At the LHC SEUs are induced

by ionizing fragments produced in nuclear interaction in the device material due to incoming high energy hadrons and thermal neutrons.

In order to ensure safe and acceptable operation of LHC electronics and any future new development, it is important to determine the expected radiation levels. For this purpose FLUKA Monte Carlo simulations are performed for the various areas of interest. However, the complex operation and layout of the LHC accelerator give rise to significant uncertainties. Dedicated radiation monitors have therefore been installed in strategic locations to provide an online measurement of the radiation levels. The main node of this system is the LHC Radiation Monitor (RadMon) [3]. During the 2010 operation these monitors have been operational and this report will present a first comparison between the measurement results and FLUKA simulations for the collimation region IR7.

1.1 IR7

At the LHC nominal operation requires a stored energy of up to 350 MJ per beam. This makes the 7 TeV proton beam highly destructive. For example, superconducting magnets at the LHC would quench if small amounts of this energy is deposited into the superconducting magnet coils [4]. A powerful and robust collimation system is therefore required to withstand the high beam intensities and to absorb unavoidable beam losses. Two of the eight long straight sections of the LHC are therefore dedicated to beam collimation. These installe at are point 3 (IR3) for momentum and point 7 (IR7) for betatron cleaning. Here protons interacting with the collimator jaws will develop into nuclear showers leading to a significant radiation load in the tunnel and close-by alcove areas. In particular IR7 is associated with high losses and it is therefore good candidate location for a first LHC application benchmark of the RadMon.

2 Procedure and methodology

This section will describe the procedure and methodology applied to perform the comparison between RadMon measurments and FLUKA simulations. It will first give an introduction to the RadMon and its application as a radiation monitor before describing the setup and assumptions for the FLUKA simulations of IR7.

2.1 The LHC Radiation Monitor (RadMon)

The RadMon radiation detection network consists of nearly 400 monitors (see figure 1) that provide an online evaluation of the radiation levels in the LHC. One of the principle ideas of the RadMon is to utilize electronic devices as radiation monitors by taking advantage of their sensitivity to radiation. The RadMon is therefore equipped with RadFETs, pin photo-diodes, and SRAM memory to measures the TID, 1-MeV equivalent neutron fluence, and the high energy hadron and thermal neutron fluence respectively. A more comprehensive description of the RadMon can be found in [3]. During the read out cycle of these memories, the data is read out byte by byte, compared to the reference (which is zero for all the standard RadMons) before the reference values is rewritten to the corresponding byte. An SEU is detected if the read out byte differs from the value of the reference byte. This approach can not detect case where one byte may contain multiple SEUs. However, due to the relatively low radiation levels and thus expected upset rate, the probability of having multiple SEUs within one byte is negligible. This report will present the result of 7 RadMons (see table 1) installed along the tunnel wall of IR7. These RadMons are in direct line of sight of the beam line and close to high beam loss points.

Figure 1: RadMon installed in the LHC. The 4 Toshiba SRAM memories can bee seen at the top of the open window of the RadMon housing.

Table 1: The table list the RadMon positions in IR7. S is the LHC longitudinal reference coordinate with the center of IR1 at S=0 and the center of IR7 at S=19994.16 (IP7). The unit of S is meter [m]. In FLUKA the reference system is defined as follows: the origin is the "interaction point" (IP7); the x and y axis are directed outgoing the LHC ring and opposite to the gravity respectively, while the z axis is orthogonal to the $x-y$ plane and directed towards positive S. The units are in centimeter [cm].

RadMon	Vertical [m]	Horizontal [m]	S [cm]	FLUKA Z [cm]
RML703	0.0	-2.3	19845	-14916
RML702	0.0	-2.3	19903	-9116
RML701	0.0	-2.3	19991	-316
RMR703	0.6	-2.3	20044	4984
RMR704	0.5	-1.7	20133	13884
RMR705	0.0	-2.3	20208	21384
RMR706	0.0	-2.3	20240	24584

At IR7 RadMons are also installed in the various UJ and RR alcoves but due to the low number of counts accumulated during the 2010 operation these are not considered in this study.

2.2 Measuring the high energy hadron fluence and the thermal neutron fluence in the LHC

To measure the high energy hadron fluence and the thermal neutron fluence the RadMon is equipped with four 4 Mbit SRAM devices from Toshiba.(0.4 μm,TC554001AF-70L). The method of using an SRAM based memory as a radiation monitor is based on that the number of SEUs induced in the memory is proportional to the incoming fluence of particles at a given energy. However, when operated in a mixed radiation environment like in the LHC, it is no longer possible to directly convert the number of SEUs into a fluence of a given particle type and energy. The approximate relationship in equation 1, and further described in [5], is therefore considered between the number of SEUs and the fluence of thermal neutrons and high energy hadrons:

$$N_{SEU}(V) = \Phi_{HEH} \cdot \sigma_{HEH}(V) + \Phi_{Th} \cdot \sigma_{Th}(V), \quad (1)$$

where $\sigma_{HEH}(V)$ and $\sigma_{Th}(V)$ are the SEU cross sections as a function of voltage determined for high energy hadrons and thermal neutrons respectively. By operating the RadMon at two different voltages with corresponding different SEU cross sections, equation 1 can be used to extract the fluence of high energy hadrons and thermal neutrons. This method is further described in [6]. The respective SEU cross sections have previously been measured in mono-energetic proton beams and a thermal neutron beam [5, 6] and are listed in table 2. During these irradiation tests a spread in the SEU response was observed between SRAM memories of the same type. An uncertainty of ±25% must therefore be applied when evaluating and comparing SEU counts of different RadMons.

Table 2: Measured SEU cross sections for thermal neutrons and high energy hadrons. The quoted errors include counting statistics and uncertainties related to the beam calibration [5, 6].

Bias	SEU cross section, σ_{SEU} (±Err) [cm^2 / bit]	
	Thermal Neutrons	High energy hadrons
3 V	$1.7 \cdot 10^{-13}$ (0.4)	$6.6 \cdot 10^{-14}$ (1.7)
5 V	$3.1 \cdot 10^{-15}$ (0.8)	$2.9 \cdot 10^{-14}$ (0.7)

2.3 FLUKA simulations of IR7

FLUKA is a well benchmarked [7, 1, 2, 8] general purpose tool for calculations of particle transport and interactions with matter, covering an extended range of applications like for example proton and electron accelerator shielding, target design, calorimetry, activation and dosimetry, cosmic ray studies, and radiotherapy. At CERN FLUKA is extensively used for machine protection issues such as energy deposition calculations and studies of material damage to accelerator elements [9]. A very detailed library of material and geometry descriptions is consequently available for accelerator elements like for example magnets and collimators. Based on this library beam lines and tunnel regions are built to study particle fluences and energy spectra relevant for SEUs in the electronics installed in various LHC alcoves. A detailed technical description of the IR7 FLUKA geometry used in this study can be found in [10].

Due to the complexity of the beam line geometry the calculation time needed to reach sufficient statistics is often a bottleneck. As the focus of this study was to compare the RadMon SEU response to the FLUKA simulation results, the transport of electrons and photons have been disabled. This effectively turns off the electromagnetic cascade which significantly reduces the calculation time. Charged hadrons are transported down to 1 MeV while neutrons are transported down to thermal energies.

2.3.1 Estimating RadMon SEU response

If the fluences of high energy hadrons and thermal neutrons are known for a given location, the SEU response of a RadMon placed in that location can be estimated by applying equation 1. Dedicated estimator/scoring regions for the IR7 RadMon locations in table 1 are therefore implemented in the FLUKA geometry as indicated in figure 2. In order to achieve reasonable statistics the regions are implemented as boxes with dimensions 40 x 40 x 40 cm^3. The boxes are filled with air. For these regions the energy spectra of all hadrons are calculated using the track length estimator (USRTRACK) of FLUKA. The fluence of high energy hadrons Φ_{HEH} and thermal neutrons are then determined by integrating over the energy interval of interest

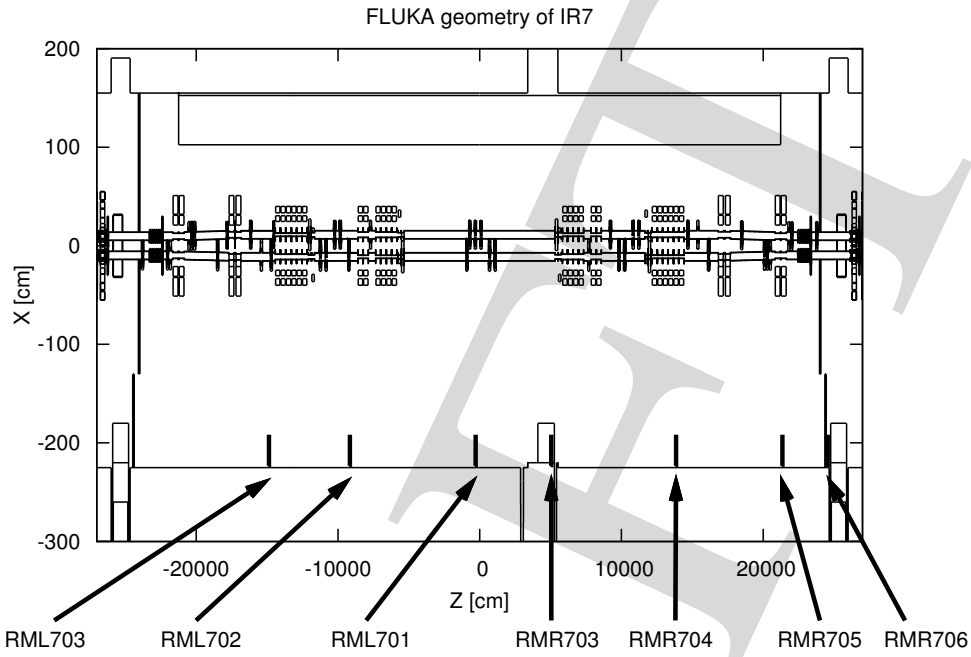

Figure 2: FLUKA geometry of IR7 indicating where the RadMon estimator/scoring regions are implemented along the tunnel wall.

according to equation 2 and 3.

$$\Phi_{HEH} = \int_{0.2\mathrm{MeV}}^{20\mathrm{MeV}} \omega(E)\,\phi_n(E)\,dE + \int_{20\mathrm{MeV}}^{\infty} \phi_{HEH}(E)\,dE, \tag{2}$$

Here $\mathrm{E_{thres}}$ = 0.2 MeV is the SEU threshold energy for neutrons and $\omega(E)$ is a weighting function for neutrons between $\mathrm{E_{thres}}$ and 20 MeV as shown in figure 3.

$$\Phi_{Th} = \int_{\mathrm{o}}^{0.5\mathrm{eV}} \phi_n(E)\,dE. \tag{3}$$

Here 0.5 eV corresponds approximately to the neutron cut-off energy in Cadmium. Below this energy Cadmium has a high neutron absorption cross section while above this energy the cross section falls off sharply. Wrapping the detector in Cadmium is therefore typically done to discriminate between the contribution from thermal and epi-thermal neutrons during irradiation tests.

A cut-off at 20 MeV is used for charged hadrons due to the increased effect of the Coulomb barrier and limited penetration below this energy. Neutrons will however contribute down to the energy threshold for nuclear interactions. To account for their decreasing effectiveness in inducing SEUs a weighting function is applied to the neutrons below 20 MeV. This weighing function is based on the results of irradiation test measurements and are further described in [5].

2.4 2010 operation: Loss terms and scaling of results

In the long straight section of IR7 movable collimators are installed on each beam line with the objective of absorbing the primary beam halo. These are referred to as primary collimators.

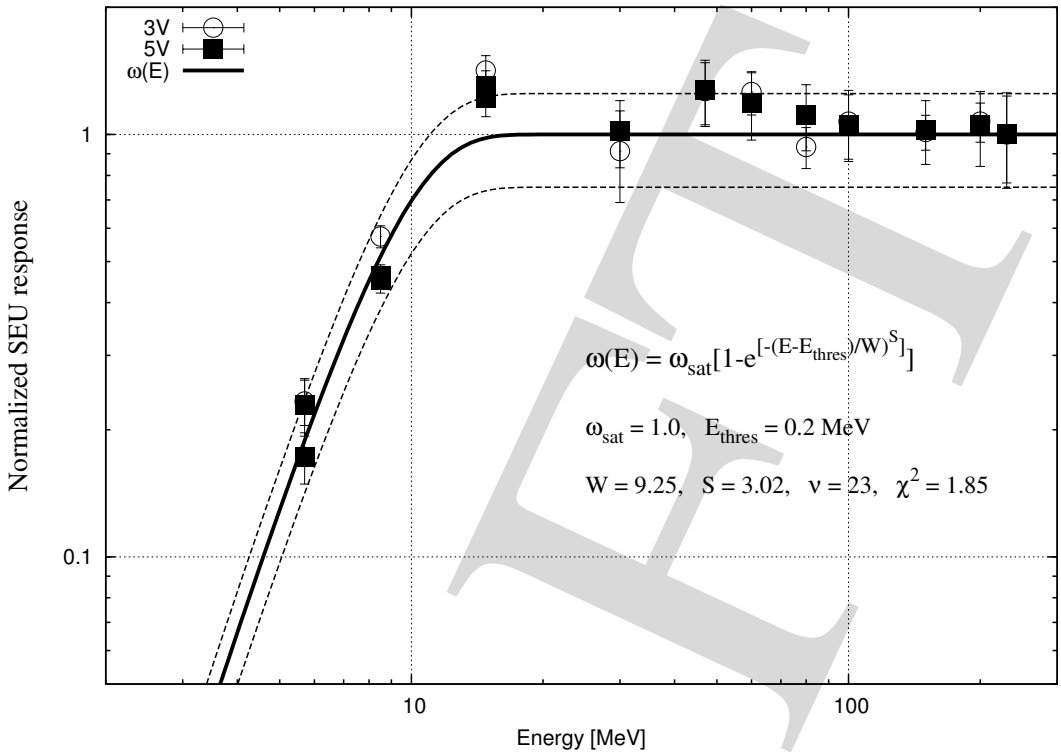

Figure 3: The neutron weighting function is based on a Weibull fit of the experimental data obtained from irradiation tests of the RadMon [5].

There are in total 3 primary collimators (vertical, horizontal, skew) on each beam line. In addition each beam line is further equipped with secondary and tertiary collimators to protect downstream elements from the secondary radiation created by the primary collimators. Concerning the electronic equipment installed in the tunnel and IR7 alcoves, all these collimators are relevant source points of radiation. To estimate the radiation load on this equipment FLUKA is used to produce and transport the hadronic showers created from the protons impinging on these collimators. For the study presented in this report the objective is to see how the results of these calculations compare with the measurement result of the RadMons installed in IR7.

2.4.1 Proton loss distribution maps

The proton loss distribution maps used as input and beam source for the FLUKA simulations are based on the particle tracking code SixTrack [11]. Loss maps are provided corresponding to the 3.5 TeV operational settings of the accelerator optics as of 2010[1] [12]. SixTrack performs particle tracking of the two proton beams around the full LHC ring and provides final loss distribution maps with information like the energy of the proton and the location coordinates of where it is interacting with the collimator. In reality the majority of losses are shared between the 3 primary collimators with some losses in secondary and tertiary collimators originating from i.e. protons passing through the primary collimators undergoing i.e. multiple coulomb scattering. Depending on the location of the RadMon, the main contribution to the SEU counts may come from one beam or one collimator only, or a combination. Seperate loss map distributions are therefore provided for the vertical and horizontal collimators of both beam 1 and beam 2. Simulating the different loss map scenarios allows to identify the main source

[1] β*=3.5m, 100 μrad half crossing angle and 3.5 TeV energy

point of radiation for each RadMon. For the simulations performed in this study the losses are assumed to be equally shared between the vertical and horizontal loss distribution scenarios. The loss map for the skew scenario was not provided but it is assumed to have a negligable effect on the final result. After the results are correctly scaled by the 2010 operational conditions (see section 2.4.2), the results of the vertical and horizontal loss distribution map scenarios are added and divided by 2 assuming an equal amount of protons lost for each scenario.

2.4.2 Scaling for 2010 operation

Based on loss map distributions provided by SixTrack, the loss location of the primary protons is sampled as a source term in the FLUKA calculations. In SixTrack loss locations are indicated as either inelastic interactions or single diffractive interactions. To avoid double counting any proton interaction subsequent of single diffractive interaction is discarded given that the interaction is within the same turn around the LHC. If a single diffractive proton makes a full turn, that is, leaves IR7 to reapear in the next turn it is should be counted. At the loss location FLUKA then forces a nuclear interaction with a certain probability (in the order of a few percent) of having a single diffractive interaction. The secondary particle distribution created from the sampled proton is then tracked in detail along the more than 500 m long geometry of the long straight section in IR7. For each of the four loss scenarios (vertical and horizontal for beam 1 and beam 2), about 2 million primaries are loaded in order to achieve reasonable statistics at the RadMon monitor locations. FLUKA outputs its results normalized to the number of sampled primary protons. These results should then be scaled to absolute values applying 2010 LHC operational conditions in order to correctly compare the results to the cumulative RadMon readings during 2010. However, there is no direct measurement providing the detailed number of lost protons for each collimator. In addition the exact distributions of particle losses at the collimators may also change between the various phases of beam operation (e.g. ramp, squeeze, stable beams). The following procedure is therefore applied to determine the total number of protons lost in IR7 during 2010 operation:

- Based on the LHC BCTs as logged in TIMBER for each fill the highest intensity for each beam in the machine is considered as "injected intensity" (see table 4).
- Immediately before the beam is dumped the last intensity value is considered as the "dumped intensity" (see table 4).
- The difference between the injected and dumped intensity is assumed to be "lost" in the machine mainly between collisions in the experiments and in collimators.
- For the number of protons lost in collisions in the experiments, the total integrated luminosity is used together with an assumed total inelastic cross section of 80 mb (see table 4).
- Subtracting the protons lost in collisions from the total number of protons lost in the machine, the remaining intensity mainly refers to protons lost in the collimators of the two collimation regions (IR3 and IR7). The fraction of lost protons in IR3 and IR7 per beam is determined based on the respective relationship between beam 1 and beam 2 for the number of protons lost in the machine (see table 4).
- The fraction of protons lost for each beam in IR7 is then determined from readings of the Beam Loss Monitors (BLMs) close to the collimators. In particular the cumulative dose at the first secondary collimator is used (see table 5).

- When injected to the LHC the protons have an energy of 450 GeV. After injection they are ramped to 3.5 TeV before stable beam conditions are declared. Analysis show that protons lost during the phase of injection and ramping only contribute to a few percent of the total losses during a fill. They are therefore not considered for the final analysis.

Table 3: Summary of injected, dumped and lost protons during 2010 LHC operation.

Proton operation				
	B1	B2	Total	
Inj. Ramped	3.13e+15	2.39e+15	5.52e+15	
Dumped	3.04e+15	2.30e+15	5.34e+15	(97 %)
Lost in machine	8.36e+13	8.83e+13	1.72e+14	(3 %)
Of lost protons				
Collisions	2.33e+13			(13 %)
Elsewhere (IR3/IR7)	1.49e+14			(87 %)

Table 4: Summary of integrated luminosity for the various experiments during during 2010 LHC operation.

Experiment	Luminosity 2010 [pb^{-1}]
ATLAS	52.04
CMS	49.55
LHCb	43.77
ALICE	0.45
Total	145.81

Table 5: The table presents the BLM readings which are used to calculate the fraction of protons lost in IR7. The cumulative dose values of the BLMs are collected for the 2010 LHC operation, that is, the same period as for when the cumulative RadMon readings are collected.

BLM identification	Beam	IR	Dose [mGy]	Fraction of total
BLMEI.06L7.B1E10_TCSG.A6L7.B1	1	7	69507	0.76
BLMEI.05L3.B1I10_TCSG.5L3.B1	1	3	22183	0.24
Total			91690	1
BLMEI.06R7.B2I20_TCSG.A6R7.B2	2	7	228275	0.85
BLMEI.05R3.B2E10_TCSG.5R3.B2	2	3	40592	0.15
Total			268867	1

The final number of protons lost in IR7 and to be used to scale the FLUKA calculation results are listed in table 6 for beam 1 and beam 2 respectively. Concerning the contribution from the horizontal and vertical loss distribution scenarios, their results are added and divided by two. This assumes that and equal amount of protons is lost for each scenario. Keep in mind however that the distribution of the losses are different and this will impact the final results compared to if only one scenario was considered.

Table 6: Final scaling factors for each FLUKA calculation scenario.

Protons lost in IR7	B1	B2
	5.48e13	6.48e13

3 Results

This section first present the FLUKA calculation results before comparing these results to the RadMon measurement results for 2010 LHC operation.

3.1 FLUKA simulations

As explained in section 2.3.1 the SEU response of a RadMon can be estimated if the fluences of high energy hadrons (Φ_{HEH}) and thermal neutrons ($\Phi_{Th.n.}$) are known. The respective results of the FLUKA calculations are therefore presented in table 7 for the various IR7 RadMon locations. In addition the table also presents fluence of neutrons (Φ_{nw}) between 0.2 MeV and

Table 7: FLUKA simulation results for the high energy hadron fluence, the weighted neutrons, and the thermal neutrons for IR7 RadMon locations.

Location	Φ_{HEH}	Err [%]	Φ_{nw}	Err [%]	$\Phi_{Th.n.}$	Err [%]
RML703	1.96e+10	0.9	4.17e+09	2.3	8.18e+10	1.1
RML702	1.24e+10	1.1	2.17e+09	3.2	3.11e+10	1.8
RML701	5.75e+09	1.7	1.51e+09	4.2	1.52e+10	2.4
RMR703	1.03e+09	2.4	1.44e+08	10.1	2.68e+09	4.2
RMR704	2.81e+10	0.8	4.04e+09	2.6	7.58e+10	1.2
RMR705	6.27e+08	4.4	2.72e+08	6.7	8.20e+09	2.8
RMR706	1.24e+07	21.9	5.10e+05	34.3	2.17e+07	21.4

20 MeV, weighted according the first part of equation 2. To better appreciate the contribution of these neutrons, their fraction (Φ_{nw}/Φ_{HEH}) of the total high energy hadron fluence is listed in table 8. Table 8 also presents the so call Risk-factor or R_{th}-factor. For the majority of devices

Table 8: The table gives the ratio of the weighted neutrons to high energy hadrons and the thermal neutrons to the high energy hadrons.

RM Loc.	Φ_{nw}/Φ_{HEH}	Err [%]	R_{th}	Err [%]
RML703	0.21	3	4.2	1
RML702	0.17	3	2.5	2
RML701	0.26	5	2.6	3
RMR703	0.14	10	2.6	5
RMR704	0.14	3	2.7	1
RMR705	0.43	8	13.1	5
RMR706	0.04	41	1.8	31

installed in the alcoves, the sensitivity to thermal neutrons is unknown. In [13] it is shown how the thermal neutron SEU cross sections can vary orders of magnitude between different types of devices. The R_{Th}-factor, giving the ratio of the thermal neutron fluence to the high-energy hadron fluence, has therefore been introduced in order to identify thermal neutron critical areas.

The radiation field maps for the high energy hadron fluence, the thermal neutron fluence, and the R_{Th}-factor is shown in figures 4 through 6. From these plots one can clearly

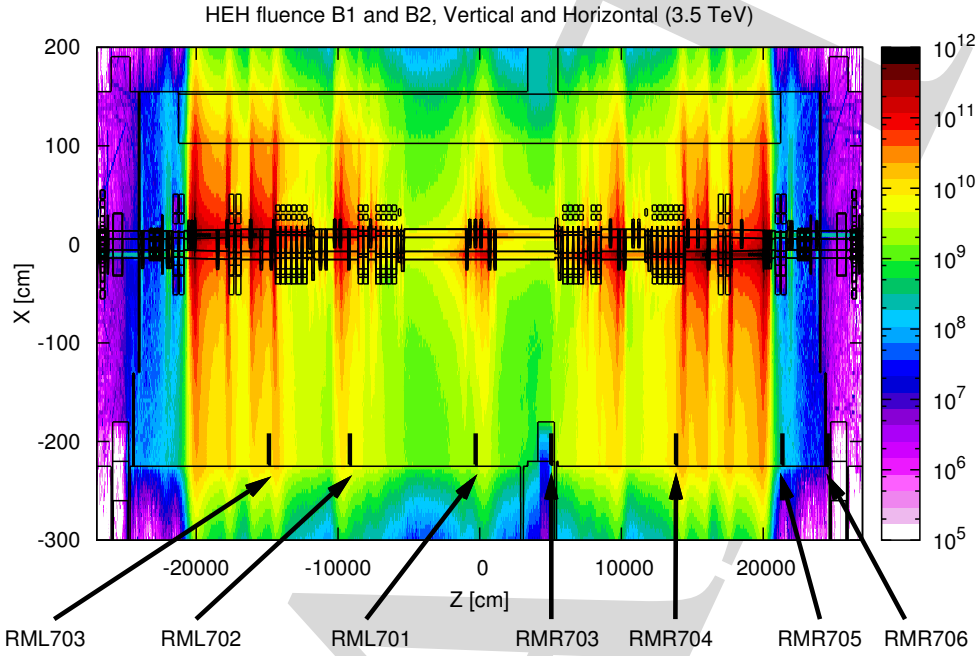

Figure 4: HEH fluence map for IR7.

see the strong gradient that exist in IR7 between the area of the primary collimators and the monitor locations. Finally, applying equation 1 the FLUKA based estimations of RadMon SEU response is presented in table 9. The respective contribution from the high energy hadrons and the thermal neutrons can be seen in the two rightmost columns. For all locations except for RMR705, the main contribution comes from the high energy hadrons. Biased at 5V the RadMon is 10 times less sensitive to thermal neutrons than high energy hadrons. In order to have the main contribution to SEU come form thermal neutrons, the thermal neutron fluence should be at least a factor 10 higher than the high energy hadron fluence. This effect can also be seen in table 8 where the FLUKA predicted R_{Th}-factor is 13. The reason for this high value comes from the location of the RMR705. As it is located immediately upstream of the primary collimators of beam 2, it sees only a small fraction of the high energy hadron showers which are mainly forward directed. In contrast the thermal neutron fluence is less directional and thus more homogeneously distributed. In reality the contribution from showers created in beam loss location further upstream should also be considered. This is expected to slightly increase the high energy hadron fluence and thus lower the R_{Th}-factor. This effect is probably partly seen in the measurement result discussed in section 3.2. The same reasoning also applies to the left side for the region immediately upstream of the primary collimators for beam 1. However, for this study no RadMons are located in this region.

3.2 RadMon measurement results and comparison to simulation

During the 2010 LHC operation the studied RadMons were all biased at 5 V and the cumulative SEU counts are presented in table 10. The measured results are in very good agreement to

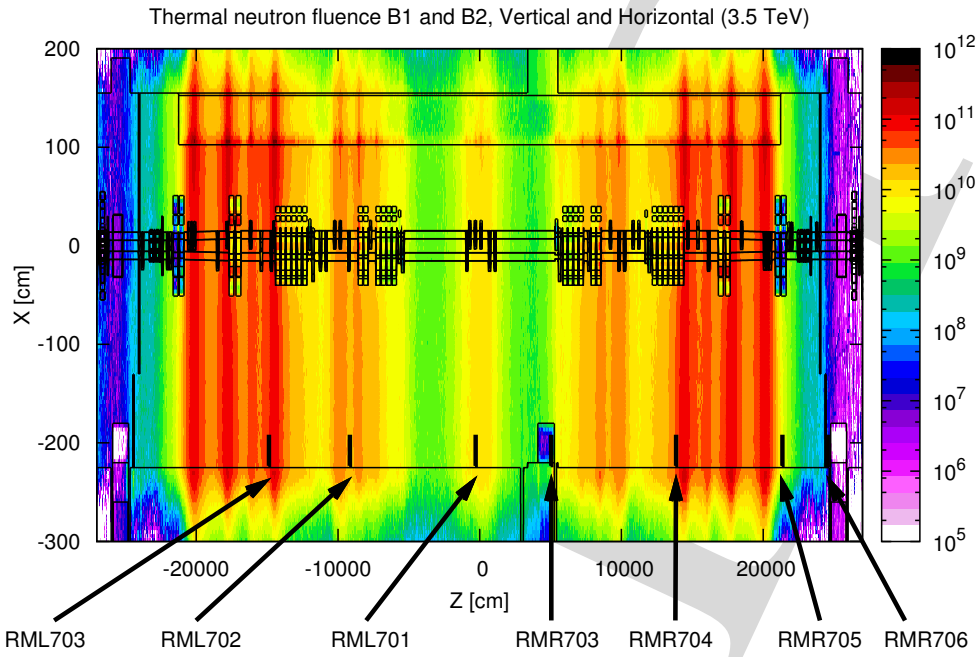

Figure 5: Thermal neutron fluence map for IR7.

the predicted values from FLUKA. Considering the complexity of the IR7 beam line these are remarkable results. However, they should be treated with care due to the associate uncertainties. The comparison is particular sensitive to the actual number of lost protons in IR7 which are used to scale the simulation results. Any changes in this number will directly change the results of all the RadMon locations. It is therefore of high importance to have a solid understanding of and procedure for how this number is extracted (see section 2.4.2). In addition the real loss distribution is not accurately known but based SixTrack simulations for a given set of beam optics settings. Additional benchmarking of the loss distribution using for example the signal response of BLMs along the beam line could therefore be of interest. However, as the BLM signal is a superposition of showers created in several nearby loss points, extracting the actual loss distribution is a difficult task. Unless all the RadMons would be placed in the close proximity of strong gradients, a shift in the loss distribution will not significantly changes the

Table 9: Expected number of accumulated SEUs as predicted by FLUKA for 2010 LHC operation. SEU-HEH is the contribution from high energy hadrons while SEU-Th.n. is the contribution from thermal neutrons

RM Loc.	SEU-Tot	Err	SEU-HEH	Err	SEU-Th.n.	Err
RML703	13800	(±2608)	9530	(±2382)	4260	(±1065)
RML702	7650	(±1560)	6040	(±1510)	1620	(±406)
RML701	3590	(±728)	2800	(±702)	791	(±198)
RMR703	641	(±130)	501	(±125)	140	(±35)
RMR704	17600	(±3555)	13700	(±3425)	3940	(±985)
RMR705	731	(±132)	305	(±77)	426	(±107)
RMR706	7	(±2)	6	(±1)	1	(±0.4)

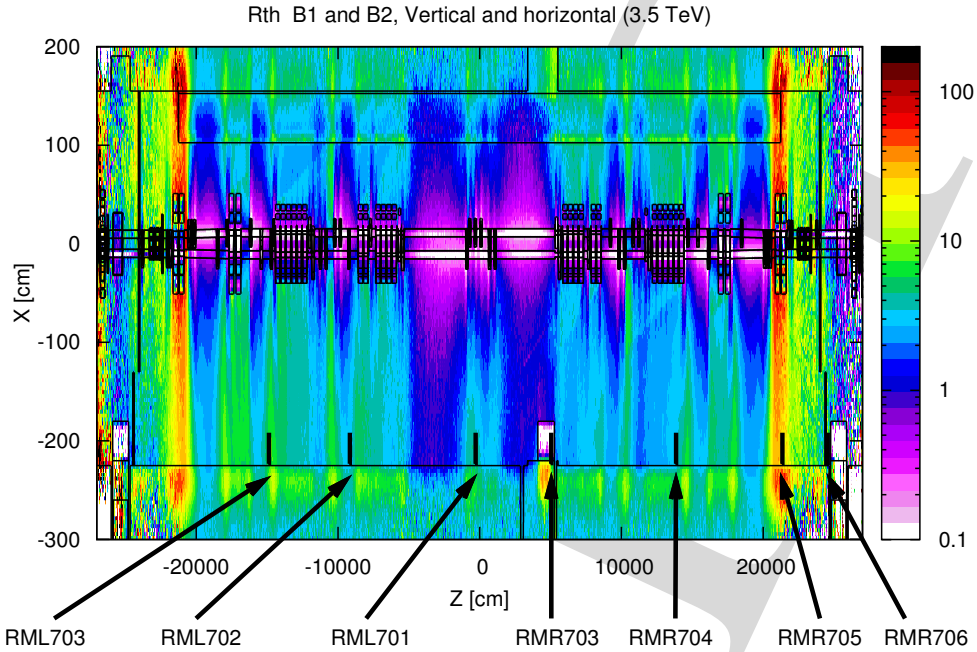

Figure 6: Rth-factor map for IR7.

overall agreement. Some RadMons would potentially see more radiation while others would see less. Another point of uncertainty is the contribution from thermal neutrons. Depending on the actual water content (concentration of hydrogen) in the concrete used in the tunnel and shielding walls, the thermal neutron fluence may change significantly. Also, equipment installed in the proximity of the RadMons may alter the thermal neutron field. Experience from e.g. CNRAD where both Au-foils and RadMon measurements (3V and 5V) were performed to extract the R_{th}-factor, shows a tendency for the simulations to overpredict the thermal neutron fluence [6]. This could partly explain the almost factor 3 higher simulation result for the RMR705 location. In fact, TLD-measurements performed in the very same location during the 2010 operation indicate an R_{th}-factor closer to 2-4 rather than 13 as predicted by FLUKA. The consequence is less significant for the other RadMon locations where the SEU counts mostly are dominated by the high energy hadrons (see table 9).

Table 10: Numberof SEUs measured by the RadMons installed in IR7 and compared to FLUKA predictions for 2010 LHC operation.

RadMon	Measurement	Err	FLUKA	Err	F/M	Err
RML703	13246	(±119)	13800	(±2608)	1.0	(±0.2)
RML702	4601	(±69)	7650	(±1560)	1.7	(±0.3)
RML701	2406	(±48)	3590	(±728)	1.5	(±0.3)
RMR703	878	(±29)	641	(±130)	0.7	(±0.2)
RMR704	17903	(±125)	17600	(±3555)	1.0	(±0.2)
RMR705	264	(±16)	731	(±132)	2.8	(±0.5)
RMR706	13	(±3)	7	(±2)	0.6	(±0.2)

4 Summary

This report has presented the first extensive comparison between simulations and RadMon SEU measurements performed in the LHC tunnel. The results demonstrate that a good agreement (within a factor 2) can be obtained even in situations with a very complex geometry, varying beam loss conditions and mixed particle fields. Furthermore, the results confirms the adequacy of using FLUKA Monte Carlo simulations to determine radiation levels relevant to radiation induced failures in the LHC electronics. On the other hand, it also shows that such good agreement can only be obtained through a thorough analysis and understanding of both the detectors' response to radiation and the source of the radiation itself.

Appendix A Beam scenario contributions

This section presents the contribution to the respective fluence and the estimated SEU response for the various simulated beam scenarios.

- B1: Contribution to the total from beam 1 including both the vertical and horizontal scenario.
- B2: Contribution to the total from beam 2 including both the vertical and horizontal scenario.
- B1_V: Contribution to the total from beam 1 considering only the vertical scenario.
- B1_H: Contribution to the total from beam 1 considering only the horizontal scenario.
- B2_V: Contribution to the total from beam 2 considering only the vertical scenario.
- B2_H: Contribution to the total from beam 2 considering only the horizontal scenario.

Table 11: This table gives the relative contribution from the various beam scenarios to total (B1+B2) high energy hadron fluence fluence.

RM Loc.	B1	B2	B1_V	B1_H	B2_V	B2_H
RML703	0.96	0.04	0.46	0.50	0.03	0.01
RML702	0.93	0.07	0.58	0.35	0.05	0.02
RML701	0.45	0.55	0.19	0.26	0.40	0.15
RMR703	0.51	0.49	0.13	0.38	0.19	0.29
RMR704	0.01	0.99	0.00	0.01	0.51	0.48
RMR705	0.07	0.93	0.02	0.05	0.34	0.59
RMR706	0.71	0.29	0.26	0.45	0.26	0.03

Table 12: This table gives the relative contribution from the various beam scenarios to total (B1+B2) thermal neutron fluence fluence.

RM Loc.	B1	B2	B1_V	B1_H	B2_V	B2_H
RML703	0.98	0.02	0.48	0.50	0.02	0.00
RML702	0.94	0.06	0.60	0.34	0.05	0.01
RML701	0.61	0.39	0.17	0.44	0.29	0.10
RMR703	0.66	0.34	0.12	0.54	0.12	0.22
RMR704	0.01	0.99	0.00	0.01	0.49	0.50
RMR705	0.02	0.98	0.00	0.02	0.32	0.66
RMR706	0.89	0.11	0.36	0.54	0.05	0.06

Table 13: This table gives the relative contribution from the various beam scenarios to total (B1+B2) weighted neutron fluence between 0.2 MeV and 20 MeV.

RM Loc.	B1	B2	B1_V	B1_H	B2_V	B2_H
RML703	0.96	0.04	0.49	0.47	0.03	0.01
RML702	0.91	0.09	0.57	0.34	0.07	0.01
RML701	0.63	0.37	0.22	0.41	0.27	0.09
RMR703	0.52	0.48	0.13	0.40	0.25	0.23
RMR704	0.01	1.00	0.00	0.01	0.51	0.48
RMR705	0.02	0.97	0.01	0.02	0.35	0.62
RMR706	0.58	0.42	0.30	0.28	0.05	0.37

Table 14: This table gives the relative contribution from the various beam scenarios to total (B1+B2) SEU response as predicted by FLUKA.

RM Loc.	B1	B2	B1_V	B1_H	B2_V	B2_H
RML703	0.96	0.03	0.47	0.50	0.01	0.03
RML702	0.93	0.07	0.59	0.35	0.02	0.05
RML701	0.49	0.51	0.19	0.30	0.14	0.37
RMR703	0.55	0.45	0.13	0.42	0.28	0.18
RMR704	0.01	0.99	0.00	0.01	0.49	0.51
RMR705	0.04	0.96	0.01	0.03	0.63	0.33
RMR706	0.74	0.26	0.27	0.47	0.03	0.23

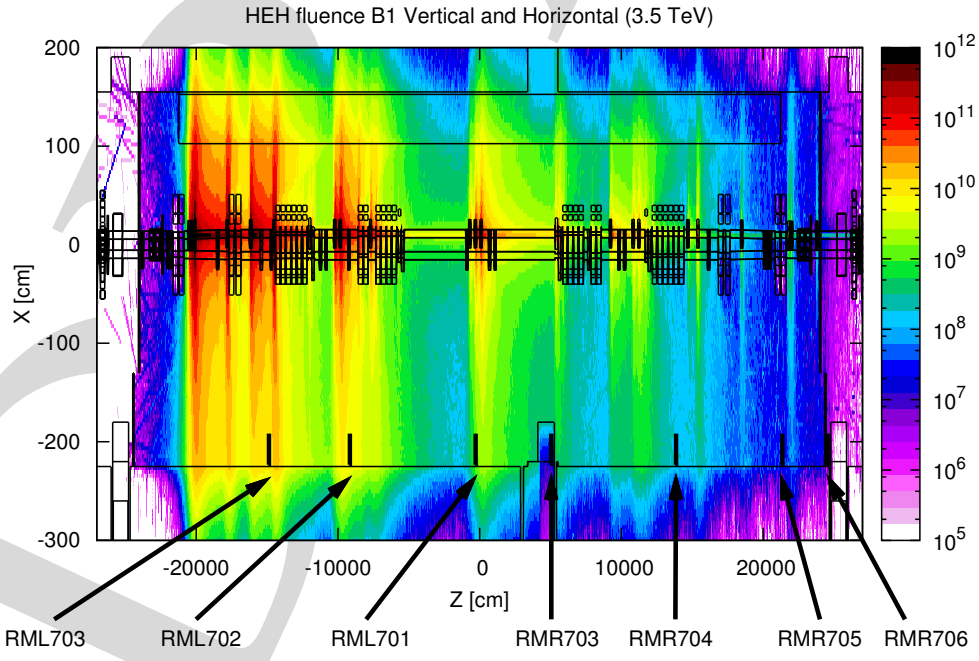

Figure 7: High energy hadron fluence map for beam 1 in IR7.

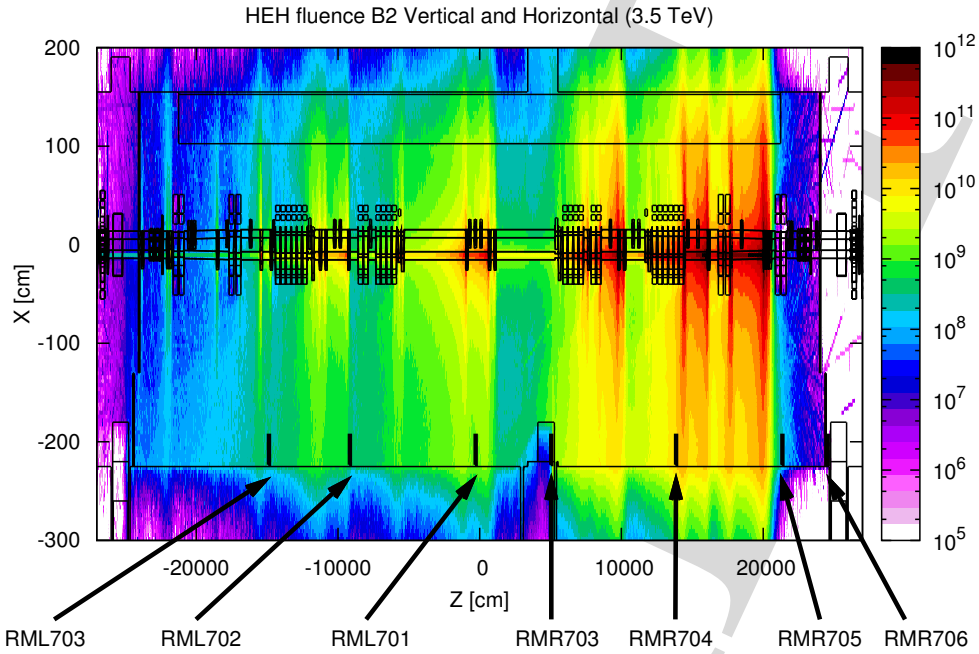

Figure 8: High energy hadron fluence map for beam 2 in IR7.

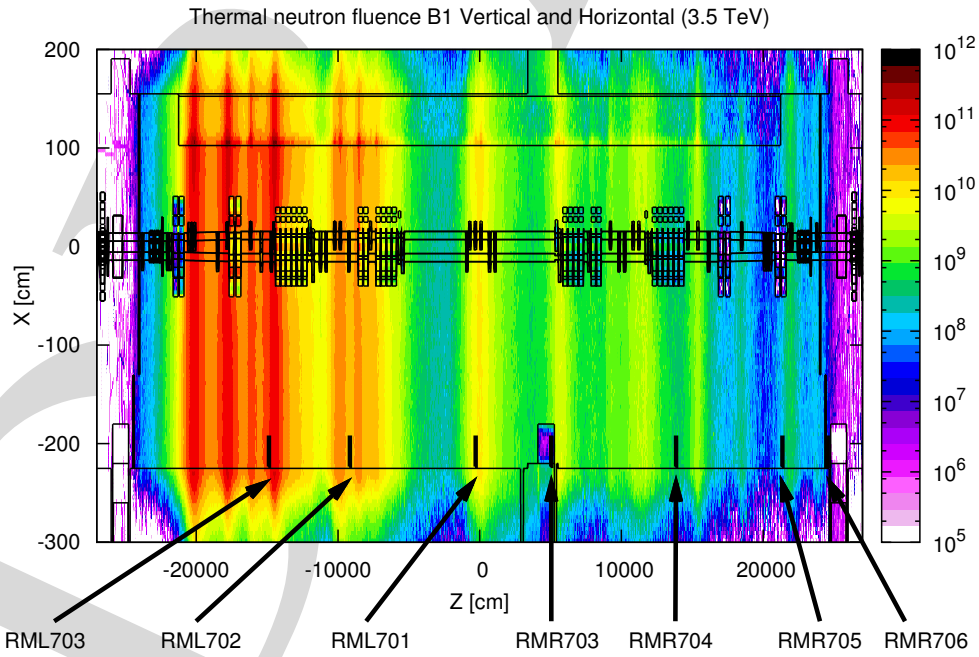

Figure 9: Thermal neutron fluence map for beam 1 in IR7.

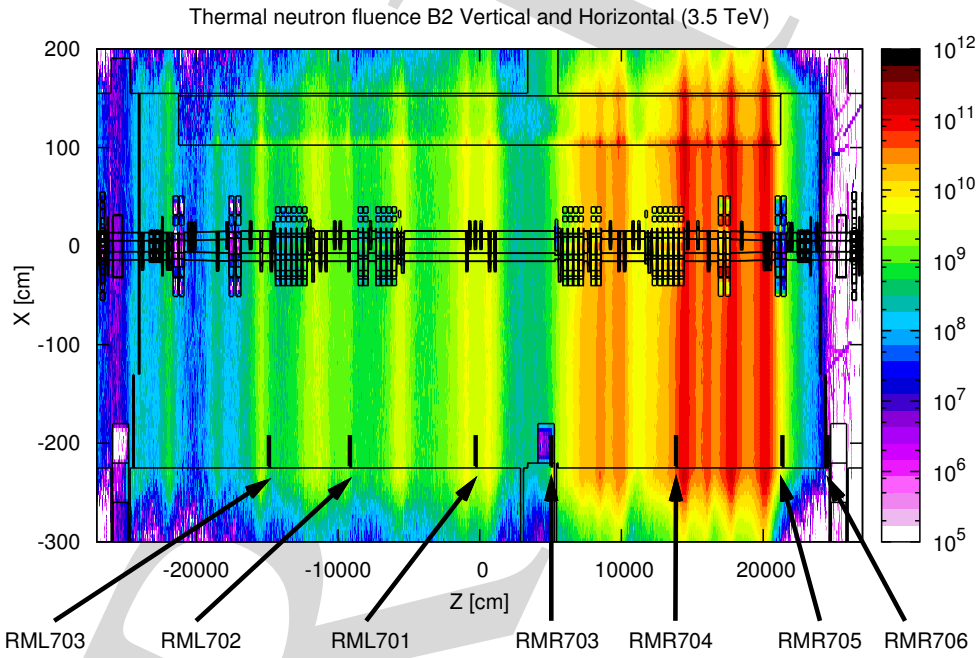

Figure 10: Thermal neutron fluence map for beam 2 in IR7.

References

[1] A. Ferrari, P. Sala, A. Fassó, and J. Ranft. *FLUKA: A multi-particle transport code*. CERN-2005-10(2005), INFN/TC_05/11, SLAC-R-773.

[2] G. Battistoni, S. Muraro, P.R. Sala, F. Cerutti, A. Ferrari, S. Roesler, A. Fassó, and J. Ranft. The FLUKA code: Description and benchmarking. *Procedings of the Hadronic Shower Simulation Workshop 2006, Fermilab 6-8 September 2006, M. Albrow, R.Raja eds., AIP Conference Proceddings 896, 31-49, (2007).*

[3] T. Wijnands, C. Pignard, and R. Tesarek. An on line radiation monitoring system for the LHC machine and experimental caverns. *12th Workshop on Electronics for LHC and Future Experiments, Conference proceedings*, 2006.

[4] O. S. Brüning, P. Collier, P. Lebrun, S. Myers, R. Ostojic, J. Poole, and P. Proudlock. *LHC Design Report*. CERN, Geneva, 2004.

[5] K. Røed, M. Brugger, D. Kramer, A. Masi, P. Peronnard, C. Pignard, and G. Spiezia. Method for measuring mixed field radiation levels relevant for SEEs in the LHC. *To be published in the proceedings of the conference on Radiation Effects on Components and Systems, Sevilla, Spain*, September 2011.

[6] D. Kramer, M. Brugger, V. Klupak, C. Pignard, K. Rø ed, G. Spiezia, L. Viererbl, and T. Wijnands. LHC RadMon SRAM detectors used at different voltages to determine the thermal neutron to high energy hadron fluence ratio. *Nuclear Science, IEEE Transactions on*, 58(3):1117 –1122, june 2011.

[7] A. Ferrari, J. Ranft, and P.R. Sala. The FLUKA radiation transport code and its use for space problems. In *1st International Workshop on Space Radiation Research and 11th Annual NASA Space Radiation Health Investigators' Workshop, Arona (Italy)*, May 2000.

[8] F. Ballarini, G. Battistoni, M. Brugger, M. Campanella, M. Carboni, F. Cerutti, A. Empl, A. Fass, A. Ferrari, E. Gadioli, M.V. Garzelli, M. Lantz, A. Mairani, A. Mostacci, S. Muraro, A. Ottolenghi, V. Patera, M. Pelliccioni, L. Pinsky, J. Ranft, S. Roesler, P.R. Sala, D. Scannicchio, G. Smirnov, F. Sommerer, S. Trovati, R. Villari, V. Vlachoudis, T. Wilson, and N. Zapp. The physics of the fluka code: Recent developments. *Advances in Space Research*, 40(9):1339 – 1349, 2007.

[9] M. Brugger, F. Cerutti, L. Lari, M. Mauri, S. Roesler, L. Sarchiapone, and V. Vlachoudis. LHC Accelerator Design Studies on the Example of Passive Absorbers. *Nuclear Technology*, 168(3):659–664, December 2009.

[10] M Brugger, F Cerutti, A Ferrari, M Magistris, M Santana-Leitner, A Tsoulou, and V Vlachoudis. Technical Description of the implementation of IR7 section at LHC with the FLUKA transport code. *CERN-AB-Note-2008-031*, Dec 2006.

[11] F. Schmidt. SIXTRACK version 1.2: single particle tracking code treating transverse motion with synchrotron oscillations in a symplectic manner; user's reference manual. Technical Report CERN-SL-94-56. CERN-SL-94-56-AP, CERN, Geneva, Sep 1994.

[12] Bruce Roderik. CERN. Personal communication, roderik.bruce@cern.ch, 2010.

[13] E. Normand, K. Vranish, A. Sheets, M. Stitt, and R. Kim. Quantifying the double-sided neutron seu threat, from low energy (thermal) and high energy (gt; 10 mev) neutrons. *Nuclear Science, IEEE Transactions on*, 53(6):3587 –3595, dec. 2006.